Suppression of the four-wave-mixing background noise in a quantum memory retrieval process by channel blocking

Kai Zhang,[1] Jinxian Guo,[1] L. Q. Chen,[1,*] Chunhua Yuan,[1] Z. Y. Ou,[1,2] and Weiping Zhang[1,†]

[1]*Quantum Institute of Atom and Light, State Key Laboratory of Precision Spectroscopy, Department of Physics, East China Normal University, Shanghai 200062, P. R. China*

[2]*Department of Physics, Indiana University-Purdue University Indianapolis, 402 North Blackford Street, Indianapolis, Indiana 46202, USA*

(Received 27 May 2014; revised manuscript received 29 July 2014; published 16 September 2014)

In a quantum memory scheme with the Raman process, the read process encounters noise from four-wave mixing (FWM), which can destroy the nonclassical properties of the generated quantum fields. Here we demonstrate experimentally that the noise from FWM can be greatly suppressed by simply reducing the FWM transition channels with a circularly polarized read beam while at the same time retaining relatively high retrieval efficiency.

DOI: 10.1103/PhysRevA.90.033823 PACS number(s): 42.65.Ky, 42.50.Gy, 42.50.Ex

I. INTRODUCTION

The ability to preserve quantum properties of the optical fields during the light-matter interaction process is crucial in quantum computing [1,2], quantum-enhanced metrology [3], quantum precision measurements [4], and photonic quantum processing [5,6]. But most light-matter interaction process, especially the transfer of the quantum fields between light and matter, will more or less bring in noise and losses to reduce and even destroy the quantum properties of the optical fields involved. The suppression of the noise and the reduction of the losses become a strong challenge in the quantum regime.

Far-detuned Raman processes [7–10] and electromagnetically induced transparency (EIT) [11–14] are the most commonly used interaction processes between photons and matter. There are usually two separate processes in which quantum fields are first transferred into some atomic excitation in an atomic system [the write process, as shown in Fig. 1(a)] and then converted back to the optical fields [the read process, as shown in Fig. 1(b)]. While the write process differs from one technique to another, the read process is basically the same: a strong near-resonant Raman read beam converts the atomic excitation to an anti-Stokes field for retrieval. The noise in the read process is more serious because it adds to the converted quantum field. The major noise usually comes from excited-state fluorescence, the four-wave mixing process (FWM), and spontaneous Raman scattering from the thermal population [15].

Generally, fluorescence can be greatly suppressed by using far-detuned fields. It has no coherent relationship with the signal fields and can be eliminated by optical frequency filters easily. The spontaneous noise can be reduced by optical pumping of atoms to ground states. The noise of FWM process, on the other hand, has its frequency exactly the same as that of the quantum signal field. Since it originates from vacuum noise, it is always there and becomes a big problem, especially for photon correlation measurements in atomic ensembles with high optical depth when the signal-photon number is small and the FWM noise is large. Fleischhauer *et al.* [15] studied theoretically this kind of FWM noise in a quantum memory process based on the EIT process. In their study, the FWM process not only introduces spontaneous decay noise into the signal fields but also provides amplification to the signal. The latter makes the FWM process even worse because it is well known that the amplification of the quantum signal is always accompanied by additional noise. Aiming at solving this problem, Walther *et al.* [16] proposed a promising scheme to eliminate the FWM noise in the write and read processes. In their proposal, instead of a traditional optical pump as shown in Fig. 1(c), polarized optical pumping is used to prepump all atoms to a single magnetic sublevel with the largest angular-momentum projection along the cell axis (called the atomic polarized population), as shown in Fig. 1(d). Then the FWM noise will be eliminated with the circularly polarized write and read beams due to the transition selection rule. Although this idea was intended for the EIT method, it should work for eliminating the FWM noise in the Raman process. Recently, however, Vurgaftman *et al.* [17] found that, in the scheme of Walther *et al.*, the write-in efficiency was greatly decreased because of the destructive interference between two hyperfine excited levels and thus hinders the usefulness of the scheme by Walther *et al.* On the other hand, since FWM noise occurs in the read process, then we address the following questions: Is necessary to prepare the atoms in the polarized states, as proposed by Walther *et al.*, for the reduction of FWM noise? Can we just modify the read process only, independent of the write process, to achieve the same goal? What about its effect on the read efficiency?

In this paper, following the idea of Walther *et al.* of using circularly polarized write and read lasers, we change in the read process the polarization of the read field from linear to circular. It shows that this change alone is enough to reduce the FWM transition channels and the FWM noise without the need to prepump atoms to a polarized state. We experimentally focus on the FWM noise in the DLCZ quantum memory scheme [18,19] and the read efficiency in the Raman read process in ^{87}Rb atomic vapor. We measure the intensity of the FWM noise in Sec. III in the Raman read process. We find that, even though we use only a normal optical pumping technique so that the atomic populations are distributed evenly among all the magnetic sublevels, the FWM noise in the Raman read process can still be greatly suppressed with a

*lqchen@phy.ecnu.edu.cn
†wpzhang@phy.ecnu.edu.cn

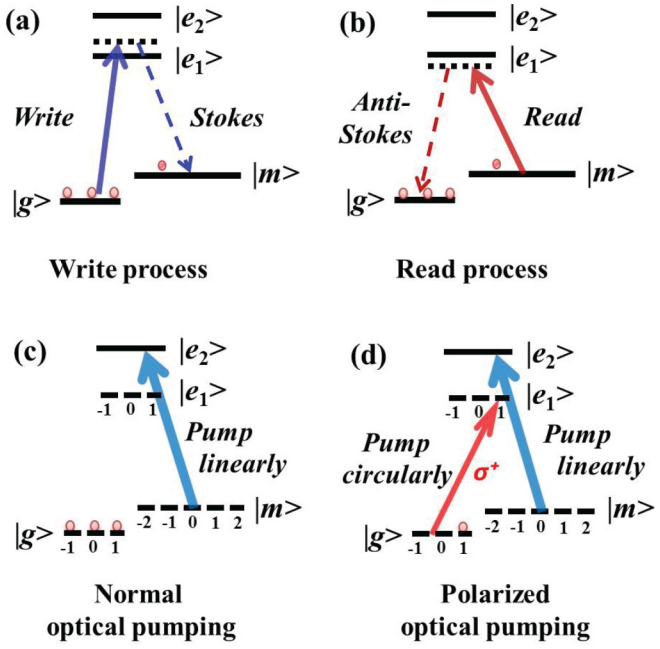

FIG. 1. (Color online) (a) Write process. (b) Read process. (c) Normal optical pumping. (d) Polarized optical pumping. The circularly polarized pump field clears the population in all magnetic sublevels but the last.

circularly polarized read beam and at the same time the read efficiency remains the same. We then obtain the read efficiency at a different atomic spin-polarized population ratio of the magnetic levels of the atomic system in Sec. IV. For the case of circularly polarized optical pumping, as the spin-polarization population ratio of atomic system increases, the write efficiency decreases but the read efficiency remains unchanged. In this case, the intensity of the FWM noise is too small to be measured under our experimental conditions. These results should be useful for the conversion of the quantum fields from their atomic storage to light.

II. EXPERIMENTAL SETUP

The experimental diagram is given in the Fig. 2. Our experiment is performed on the ^{87}Rb atoms contained in a

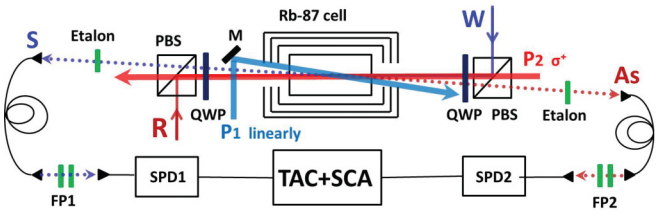

FIG. 2. (Color online) Schematic experimental setup. W: write; S: Stokes; R: read; AS: anti-Stokes; P_1: linearly polarized pump; P_2: circularly polarized pump; M: mirror; QWP: zero-order quarter-wave plate; PBS: polarizing beam splitter; FP1 and FP2: Fabry–Perot cavities; SPD1 and SPD2: single-photon detectors; TAC: time-amplitude converter; SCA: single channel analyzer. The read laser counterpropagates and overlaps with the write laser.

5-cm-long paraffin-coated cell without buffer gas. The cell is heated to 75 °C with a bi-filar resistive heater. The atomic levels and the laser frequencies are given in Figs. 1(a)–1(d). We use the Raman process to write and read the quantum states to and from the atoms. Before the experiment, the atomic ensemble needs the initial preparation, i.e., the optical pumping process (OP), to reduce the loss of subsequent generated signal fields and enhance subsequent interaction efficiency. As shown in Figs. 1(c) and 1(d), there are two kinds of initial preparation processes as needed: the first one is the normal OP to initially populate atoms at the hyperfine ground state $5\,^2S_{1/2}(F=1)$. This is achieved by an 80-μs-long pulse from a 200 mW P_1 laser with linear polarization, its frequency is resonant on the transition $5\,^2S_{1/2}(F=2) \rightarrow 5\,^2P_{3/2}$. The depopulation degree of the $|m\rangle$ state $[5\,^2S_{1/2}(F=2)]$ is smaller than 2% in the experiment. The other initiation process is the polarized optical pumping, which requires two 80-μs-long laser beams P_1 and P_2 simultaneously. P_1 emits at 780 nm with linear polarization and is resonant on the transition $5\,^2S_{1/2}(F=2) \rightarrow 5\,^2P_{3/2}$ to prepare all atoms in the ground state $5\,^2S_{1/2}(F=1)$. P_2 is at 795 nm with σ^+ polarization and is resonant on the transition $5\,^2S_{1/2}(F=1) \longrightarrow 5\,^2P_{1/2}(F'=1)$ to pump atoms from the magnetic sublevels $5\,^2S_{1/2}(F=1,m_F=-1,0)$ to $5\,^2S_{1/2}(F=2)$. So the two optical pumping beams P_1 and P_2 will initially populate most atoms at $5\,^2S_{1/2}(F=1,m_F=1)$ with a few at $5\,^2S_{1/2}(F=1,m_F=-1,0)$. The atomic polarization population ratio of $5\,^2S_{1/2}(F=1,m_F=1)$ to $5\,^2S_{1/2}(F=1,m_F=-1,0,1)$ changes with the power of the P_2 beam. After the OP pulses, we send a write laser into the cell to generate the atomic spin excitation and the corresponding Stokes photons through the spontaneous Raman process. The write laser has a power of several milliwatts with a duration of 100 ns and is tuned to the $5\,^2S_{1/2}(F=1) \rightarrow 5\,^2P_{1/2}(F=2)$ transition with a detuning of +0.5 GHz. The intensity of Stokes photons is controlled at single-photon level. We use three filters to separate the Stokes photons from the write beam. The first is a polarizing beam splitter to filter out most of the write photons with a 40 dB extinction ratio. The second is an optical etalon to filter the leaked write photons at 30 dB with a transmission of the Stokes photons at 80%. At last, the signal photons are coupled into a single-mode fiber (SMF) at 1 degree angle from the write beam to spatially filter the leaked write photons further. The Stokes photons after SMF are sent into a Fabry–Perot (FP) cavity for the analysis of the frequency and intensity of the Stokes beam and whatever is left after the filtering for the write beam with a single-photon detector, a time-to-amplitude converter, and a single-channel analyzer. The overall collection efficiency of the Stokes photons is about 25%.

In the write process, the detection of a Stokes photon means the successful creation of a collective atomic excitation. In the subsequent read process, a read pulse with a duration of 200 ns is sent into the atomic cell to convert the atomic excitation into the anti-Stokes photon. The read laser is red-detuned with $\Delta = -0.8$ GHz from the transition $5\,^2S_{1/2}(F=2) \rightarrow 5\,^2P_{1/2}(F'=1)$ and the power is strong at about 60 mW. Similar to the Stokes photons in the write process, the anti-Stokes photons are collected by another single-mode fiber and analyzed with a single-photon detector (SPD), a time-to-amplitude converter (TAC), and a single-channel analyzer (SCA) after the FP

cavity. The polarization of the write and read lasers are controlled by two quarter-wave plates (QWPs) at each end of the cell: the two lasers are linearly polarized without the QWPs but circularly polarized with the QWPs.

III. FOUR-WAVE-MIXING NOISE

In this section, we focus on the FWM noise that occurs concurrently in the Raman read process. We measure the anti-Stokes photons in two cases and compare these results to get the intensity information about the FWM noise. First, we measure the anti-Stokes signal by using a linearly or circularly polarized read beam without the write process, i.e., after the normal OP, the read beam is directly sent into the cell without applying the write beam. Because there is no atomic spin wave before the read beam enters the cell, the measured anti-Stokes signals all come from the FWM process. Second, we measure the anti-Stokes signal by using a linearly or circularly polarized read beam after the write process under same experimental conditions, in this case there is the atomic spin wave prebuilt by the write laser in the cell before the read pulse. The measured anti-Stokes signal is a mixture of the FWM noise and the real readout signal.

Figure 3 is the spectrum of the anti-Stokes from the scan of the FP cavity without the write process. Because the free spectral range of the FP cavity is only 1.1 GHz, which is smaller than the 6.8 GHz separation between the read and

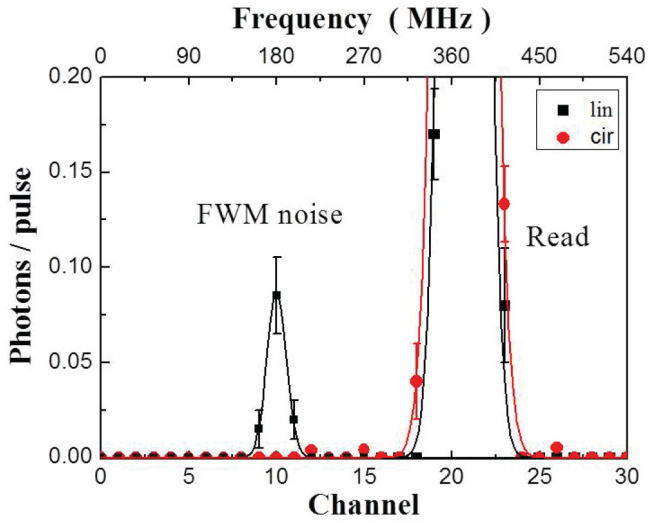

FIG. 3. (Color online) The spectrum of the anti-Stokes signal from the scan of the FP cavity without write process. The FWM noise with linearly polarized read beam is shown as black squares and the circularly polarized read beam is shown as red dots. The solid lines connect the data points in a smooth fashion for visual guidance. The x axis is the channel of SCA and stands for the frequency, with 18 MHz per channel. The Fabry–Perot cavity is scanned by a triangular voltage with a frequency f of 5 Hz that is synchronized with the pulse sequence. The FSR is about 1.1 GHz. The time window per channel, ΔT_c, is set to 0.5 ms. The pulse number can be obtained by $N_{\text{pulse}} = \Delta T_c f t/T$. T is the period of the pulse sequence and t is the integral time. The y axis stands for the intensity of signal expressed in photons per pulse: $N_{\text{photon}}/N_{\text{pulse}}$. N_{photon} is the total number of photons detected during the time window.

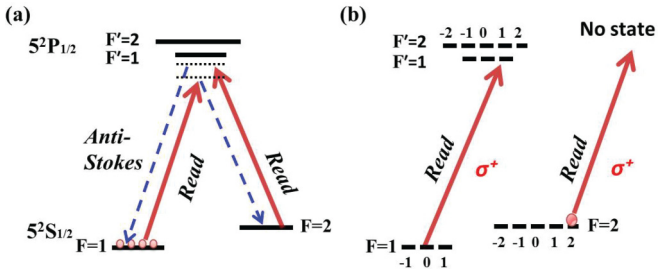

FIG. 4. (Color online) (a) The generation of FWM noise during the read process based on Raman scattering with normal optical pumping and using a linearly polarized read beam. (b) The suppression of FWM noise based on the scheme of Walther *et al.* in which atoms are prepumped into the highest magnetic sublevel and the read beam is circularly polarized. The circularly polarized read beam cannot couple $|5\,^2S_{1/2}, F = 2, m_F = 2\rangle$ to the excited state $|5\,^2P_{1/2}, F' = 1,2\rangle$.

the anti-Stokes beam, the relative position of the two peaks is rather strange (they belong to different orders of FP fringes). Nevertheless, they can be identified as labeled. The power of the read beam is so strong that it pumps the atoms at the ground state up to the m state even at large mismatched detuning and then back to the ground state, completing the four-wave mixing process, as shown in Fig. 4(a). Since there is no atomic population in the m state from the write process with a write laser, the detected anti-Stokes photons are all from the FWM noise of the read beam due to spontaneous decay in FWM. Note that this FWM noise cannot be eliminated because it has the same frequency as the real readout quantum fields when there is a write beam. The black squares in Fig. 3 show the frequency spectrum of the anti-Stokes photons when using a linearly polarized read beam. The intensity of the anti-Stokes noise is measured at about 0.08 photon/pulse. After considering the collection efficiency of the SMF and FP cavity, the anti-Stokes noise is 0.36 photon/pulse, which is comparable to the intensity of the single-photon-level quantum field. The red dots in Fig. 3 show the result of the circularly polarized read beam upon adding the quarter-wave plates at each end of the cell. Other conditions, such as the power, frequency, and duration, are the same as for the linearly polarized case. The measured anti-Stokes photon in this case is largely suppressed to under 0.01 photon/pulse, which is the dark counts of the single-photon detector. Such FWM noise at this level can be neglected compared with the intensity of the quantum field. So, the FWM noise from spontaneous decay can be greatly suppressed by using the circularly polarized read beam under our present experimental conditions. Note that here we do not prepump the atoms to the polarized states. We believe that the FWM noise can be further suppressed with the atoms initially prepared in the spin-polarization states on the basis of the scheme by Walther *et al.* [16], as shown in Fig. 4(b). We cannot confirm this because its intensity is too weak to be detected in our experiment. But this will lead to reduced write efficiency as shown by Vurgaftman *et al.* [17] and by our experiment to be described later.

We can understand the above results with a theoretical analysis as follows: The intensity of the FWM signal is determined by the elements of a third-order nonlinear susceptibility tensor

$\chi^{(3)}$ [20], so the rate of FWM at frequency ω can be found as

$$R_{\mathrm{FWM}}(\omega) = \left| \sum_{gklm} \chi^{(3)}_{gklm}(\omega) \right|^2, \quad (1)$$

and $\chi^{(3)}_{gklm}$ has the form of

$$\chi^{(3)}_{gklm}(\omega) = \frac{\mu_{kg}\mu_{mk}\mu_{lm}\mu_{gl} N \rho^0_{gg}}{(\omega_{kg} - \omega_p - i\Gamma_{kg})(\omega_{lg} - \omega - i\Gamma_{lg})} \times \frac{1}{(\omega_{mg} + \omega_s - \omega_p - i\Gamma_{mg})},$$

where N is the atomic number density, and μ_{ij} denotes the ij matrix element of the dipole operator and has been presented by Steck [21]. The summation refers to all possible FWM channels. It is worth recalling that the subscripts of the matrix element denote the magnetic sublevels in the initial, the intermediate, and the final states. Accordingly, ρ^0_{gg} is the population of the initial atoms in one of the magnetic sublevels. As seen in the Appendix, there is a significant reduction in the number of the transition channels for the FWM process with a circularly polarized read beam as compared to the case with a linearly polarized read beam, leading to a decrease in the rate of FWM by a factor of about 16 (the detailed calculation of the FWM transition rate is given in the Appendix). That is to say, the intensity of the anti-Stokes photons generated from the FWM process with the σ^+ read laser is about 6% of that with the linearly polarized read laser with our frequency conditions. In our experiment, the FWM noise with the linearly polarized read laser is 0.08 photon/pulse and, by theory, it should be reduced to 0.005 photon/pulse by using σ^+ read laser. Experimentally, we find it below the dark count level of 0.01 photon/pulse when using σ^+ read laser. So, our experimental data have demonstrated such a suppression effect.

Next, we send in the write beam to measure the FWM noise in the Raman read process with the presence of the atomic excitation at the m state produced by the write-in process. The frequency spectrum is given in Fig. 5. The black squares are for the case of linearly polarized write and read beams while the red dots are for the case of the σ^- write beam and σ^+ read beam (we cannot use a linearly polarized write beam in the latter case because of the experimental configuration). In both cases, the atoms are optically pumped by linearly polarized light and the intensities of the Stokes photons generated in the write process are controlled to be equal to 0.50 photon/pulse, as shown in Fig. 5(a). So the intensity of the atomic excitations in the cell, which is correlated to the Stokes field, is same before the read process. Notice that we need to increase the power of the circularly polarized write beam by about a factor of 2.5 in order to keep the intensity of the Stokes signal at 0.5 photon/pulse because of the decrease of the write efficiency with the circularly polarized write laser. For the read process shown in Fig. 5(b), we can see that the anti-Stokes photons is 0.22 photon/pulse with a linear polarized read beam but is 0.14 photon/pulse with a σ^+ read beam. The difference is about 0.08 photon/pulse, equal to the intensity of the FWM noise in Fig. 3 without the write process. There are two kinds of noise in the FWM process coming from spontaneous decay and amplification of the signal [15]. That is to say, besides the FWM noise from spontaneous decay, there may be additional noise generated from the amplification effect of the existing atomic excitation. Obviously, from Fig. 5, the intensity difference is all from the FWM noise from spontaneous decay

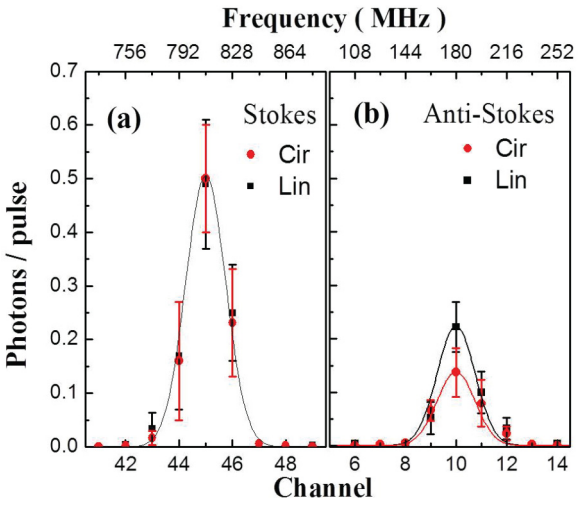

FIG. 5. (Color online) The spectrum from the scan of the FP cavity for (a) the Stokes field in the write process and (b) the anti-Stokes field in the read process. The cases for linearly and circularly polarized read beams are marked as black squares and red dots, respectively. The solid lines connect the data points in a smooth fashion for visual guidance. The labels for the axes are the same as for Fig. 3.

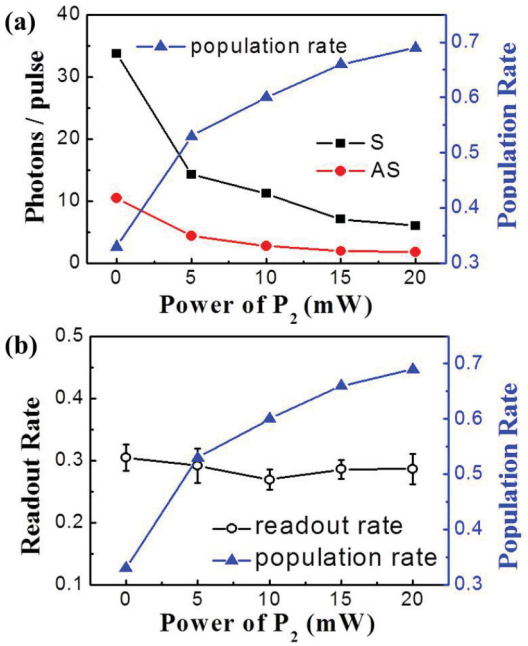

FIG. 6. (Color online) (a) Stokes (squares) and anti-Stokes (solid circles) photons number per pulse generated in the write and read processes with circularly polarized write and read beams and atomic polarized population ratio of the magnetic sublevels (triangles) as a function of the power of laser P_2. (b) The corresponding retrieve rate for the case of panel (a).

and the noise from the amplification effect is very small here. The 0.14 anti-Stokes photon/pulse in the σ^+ read laser case is the real readout anti-Stokes signal due to the atomic excitation in the m state produced in the write-in process, which is equal to the total anti-Stokes photons minus the FWM noise of 0.08 photon/pulse in the case of a linearly polarized read laser. This photon level corresponds to 28% read efficiency. This demonstrates that the retrieval efficiency is not affected by the change of the polarization of the Raman read lasers.

Note that, in the above experiment, the atoms are pre-pumped to all magnetic sublevels. As we mentioned earlier, the FWM noise can be further reduced if we use a polarized optical pump to prepump atoms to a single magnetic sublevel with the largest angular-momentum projection along the cell axis. Even though we did not observe the reduction in our experiment because of the smallness of the effect, we believe when the power of the read field is stronger [22] or the optical depth is much larger [23] than for our experiment, the FWM noise will be large enough and it will be necessary to apply the technique of polarized optical pumping suggested by Walther *et al.* From the work by Vurgaftman *et al.* [17], we learned that the write-in efficiency is reduced. Then, what happens

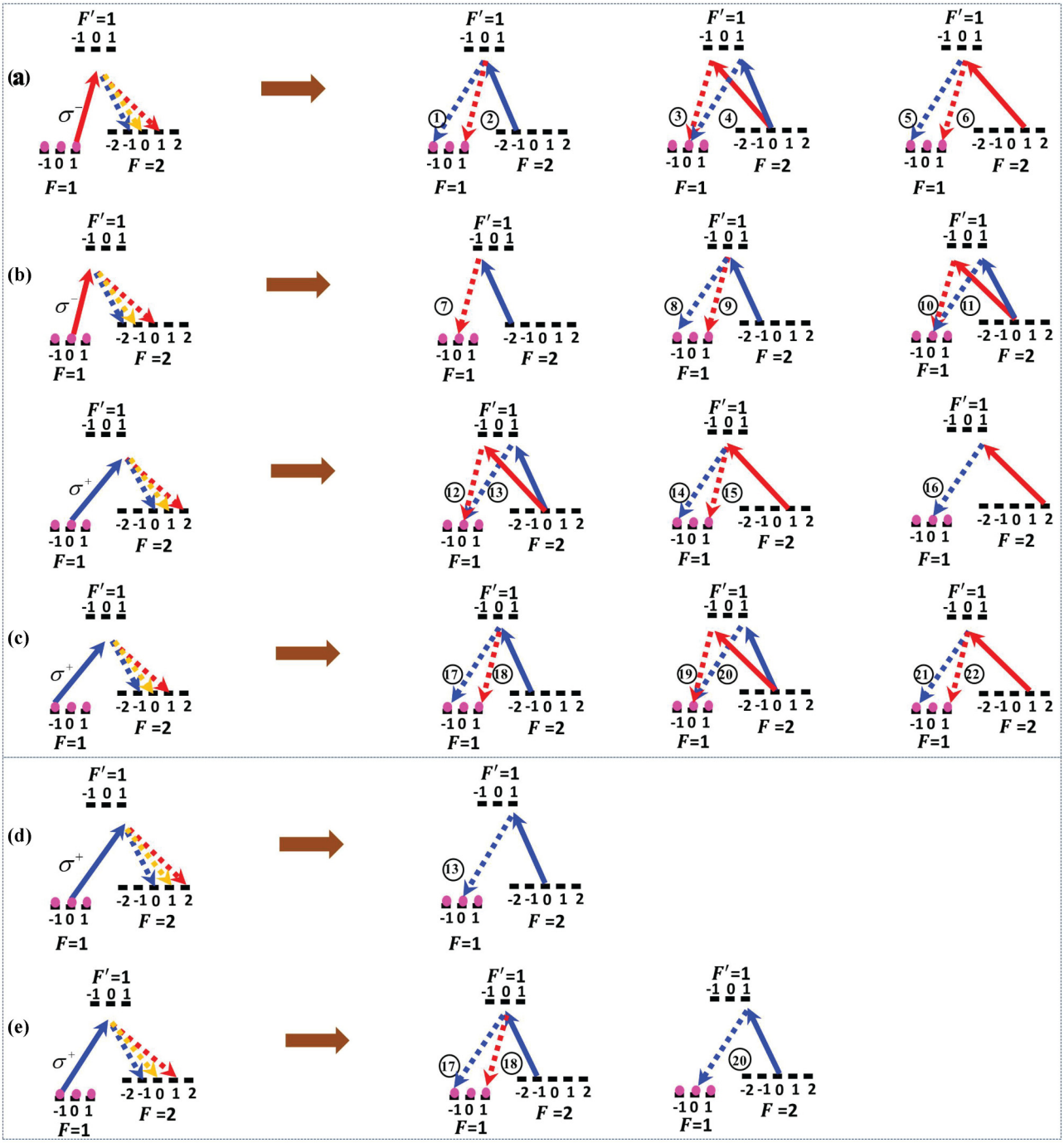

FIG. 7. (Color online) The FWM transition channels starting from the state $5\,^2S_{1/2}(F=1)$ with (a)–(c) linearly polarized and (d), (e) circularly polarized read laser. Blue is σ^+ polarization, red is σ^- polarization, and yellow is π polarization.

to the readout efficiency if the atoms are prepared in the spin-polarized states?

IV. RETRIEVAL EFFICIENCY

Now we add the P_2 prepump laser to prepare the atoms in a polarized state. In Fig. 6(a) we give the intensity of the Stokes photons (black squares) with a σ^- Raman write laser and the anti-Stokes photons (solid red circles) with a σ^+ Raman read laser as a function of the power of the P_2 pumping field. We also plot the measured atomic polarized population ratio (triangles; with the scale on the y axis on the right side) at different P_2 power. The polarized population ratio of the atomic system increases with the power of the P_2 OP beam. From Fig. 6(a), as the power of the P_2 beam increases, the intensity of the Stokes photons decreases, which agrees with the experimental and theoretical results reported in Ref. [17]. At the same time, the intensity of the readout anti-Stokes photons decreases with the write Stokes photons as well. The ratio of the anti-Stokes to the Stokes gives the retrieval efficiency, which is plotted in Fig. 6(b) as a function of the powers of the P_2 pumping field. For comparison, we also plot the measured atomic polarized population ratio in Fig. 6(b). It can be seen that the retrieval efficiency remains at about 30% as the polarized population ratio increases. Figure 6 indicates that the polarized population has a large effect on the generation of the Stokes photon but has almost no effect on the retrieval efficiency.

To understand the results above, we notice that, in an optically thick atomic medium, the anti-Stokes signal generated in the read process can be written as [24]

$$\hat{E}_{\mathrm{AS}} = -\frac{\Omega_R}{g\sqrt{N}}\hat{S}_{\mathrm{spin}}, \tag{2}$$

where N is the number of atoms, $\hat{S}_{\mathrm{spin}}$ is the collective atomic spin excitation created in the write process, $\Omega_R = \mu E_{\mathrm{read}}$ is the Rabi frequency of the read laser with E_{read} as the amplitude of the read laser and μ as the dipole moment of the $|e\rangle$-$|m\rangle$ transition. g is the atom-light coupling constant which is also proportional to μ. Thus, from Eq. (2), we find that the retrieval efficiency $|E_{\mathrm{AS}}|^2/|S_{\mathrm{spin}}|^2$ is independent to the dipole moment μ, which can be changed by the variation of the polarized population ratio in our experiment. This is so because, in essence, the read process can be considered as a kind of stimulated-emission process based on the collective atomic excitation [24,25]. In contrast, the write process is spontaneous Raman scattering and the intensity of the Stokes signal depends on the dipole moment μ. This is the reason why the intensity of the Stokes photons decreases with the atomic polarized population ratio while the retrieval efficiency is kept constant.

V. CONCLUSIONS

In summary, we measured the FWM noise in the read process with Raman process. Our experimental results show that the intensity of the FWM noise is comparable to that of the quantum signal when the read beam is linearly polarized but can be reduced greatly just by using a circularly polarized read field. The retrieval efficiency remains the same while the noise decreases. For the FWM noise reduction, it is not necessary to follow the proposal by Walther *et al.* of preparing atoms in a polarized state. Furthermore, when the scheme of Walther *et al.* is applied, the retrieval efficiency is unchanged for different polarized states and the intensity of the FWM noise is too small to be measured in our experimental system. Our work should be useful for the retrieval of quantum fields in atoms in the protocols based on light-atom interactions for quantum memory and precision measurement.

ACKNOWLEDGMENTS

This work is supported by the National Basic Research Program of China (973 Program Grant No. 2011CB921604, the National Natural Science Foundation of China (Grants No. 11274118, No. 11004058, No. 11474095, No. 11129402, No. 11234003, and No. 11204085), and is supported by the Innovation Program of the Shanghai Municipal Education Commission (Grant No. 13ZZ036) and the Fundamental Research Funds for the Central Universities.

APPENDIX: FOUR-WAVE-MIXING CHANNELS

The FWM transition channels and transition rate with $5\,^2P_{1/2}(F' = 1)$ as excited state are given in Fig. 7 and Table I, respectively. The transitions of the excited state $5\,^2P_{1/2}(F' = 2)$ are similar but are not shown here because of the large number (84) of possible channels. In our experiment, almost all atoms are initially pumped at $5\,^2S_{1/2}(F = 1)$ by linearly polarized OP field, few atoms populate at $5\,^2S_{1/2}(F = 2)$. Although the read laser is near resonant on the transition $5\,^2S_{1/2}(F = 2) \rightarrow 5\,^2P_{1/2}(F' = 1)$, all FWM transitions start from $5\,^2S_{1/2}(F = 1)$. In the calculation, all experimental conditions, such as polarization of the fields, detuning frequency, and frequency difference between energy levels $5\,^2S_{1/2}(F = 1,2)$, are considered.

Figures 7(a)–7(c) are transitions with linearly polarized read laser, which can be treated as a superposition of σ^+ polarized and σ^- polarized lasers. As shown in Figs. 7(a)–7(c), with the linearly polarized read, there are 22 possible FWM transition channels. The $\chi^{(3)}(\omega)$ of each channel is listed in Table I, expressed as multiples of $C = (\langle J = 1/2 \| er \| J' =$

TABLE I. The $\chi^{(3)}(\omega)$ of each FWM transition channels with $5\,^2P_{1/2}(F' = 1)$ as excited state. It is expressed as multiples of $(\langle J = 1/2 \parallel er \parallel J' = 1/2\rangle)^4$.

Channel	$10^{-24}\chi^{(3)}(\omega)$	Channel	$10^{-24}\chi^{(3)}(\omega)$
1	$0.17 - 3.42i$	12	$0.06 - 1.14i$
2	$-0.17 + 3.42i$	13	$-0.06 + 1.14i$
3	$-0.11 + 2.28i$	14	$-0.17 + 3.42i$
4	$0.11 - 2.28i$	15	$0.17 - 3.42i$
5	$0.17 - 3.42i$	16	$-0.34 + 6.84i$
6	$-0.17 + 3.42i$	17	$-0.17 + 3.42i$
7	$-0.34 + 6.84i$	18	$0.17 - 3.42i$
8	$0.17 - 3.42i$	19	$0.11 - 2.28i$
9	$-0.17 + 3.42i$	20	$-0.11 + 2.28i$
10	$-0.06 + 1.14i$	21	$-0.17 + 3.42i$
11	$0.06 - 1.14i$	22	$0.17 - 3.42i$

$1/2\rangle)^4$ [21]. The total rate of the FWM process is the summation of all 22 transitions as given in Eq. (1). The FWM rate $R^L_{\mathrm{FWM}}(\omega)$ is $1.87 \times 10^{-46}C$ in the linear-polarization case. Figures 7(d) and 7(e) are the transitions with a σ^+ polarized read laser and there are only four possible transition channels because of the selection rule. The corresponding FWM rate $R^C_{\mathrm{FWM}}(\omega)$ is $1.17 \times 10^{-47}C$. If we include the transitions through the excited state $5\,^2P_{1/2}(F' = 1,2)$, there are total of 106 transition channels in the linear-polarization case but only 21 channels in the circular-polarization case. Considering the experimental conditions, the corresponding $R^L_{\mathrm{FWM}}(\omega)$ is $1.7 \times 10^{-46}C$ and $R^C_{\mathrm{FWM}}(\omega)$ is $1.06 \times 10^{-47}C$, respectively. So, the reduction of transition channels leads to a decrease in the FWM rate by a factor of about 16.

[1] E. Knill, R. Laflamme, and G. J. Milburn, Nature (London) **409**, 46 (2001).

[2] Samuel L. Braunstein and Peter van Loock, Rev. Mod. Phys. **77**, 513 (2005).

[3] I. Afek, O. Ambar, and Y. Silberberg, Science **328**, 879 (2010).

[4] Min Xiao, Ling-An Wu, and H. J. Kimble, Phys. Rev. Lett. **59**, 278 (1987).

[5] M. A. Broome, A. Fedrizzi, S. Rahimi-Keshari, J. Dove, S. Aaronson, T. C. Ralph, and A. G. White, Science **339**, 794 (2013).

[6] J. B. Spring, B. J. Metcalf, P. C. Humphreys, W. S. Kolthammer, X.-M. Jin, M. Barbieri, A. Datta, N. Thomas-Peter, N. K. Langford, D. Kundys *et al.*, Science **339**, 798 (2013).

[7] Julien Laurat, Hugues de Riedmatten, Daniel Felinto, Chin-Wen Chou, Erik W. Schomburg, and H. Jeff Kimble, Opt. Express **14**, 6912 (2006).

[8] Shuo Jiang, Xiao-Ming Luo, Li-Qing Chen, Bo Ning, Shuai Chen, Jing-Yang Wang, Zhi-Ping Zhong, and Jian-Wei Pan, Phys. Rev. A **80**, 062303 (2009).

[9] A. E. Kozhekin, K. Molmer, and E. Polzik, Phys. Rev. A **62**, 033809 (2000).

[10] K. F. Reim, P. Michelberger, K. C. Lee, J. Nunn, N. K. Langford, and I. A. Walmsley, Phys. Rev. Lett. **107**, 053603 (2011).

[11] S. E. Harris, Phys. Today **50**(7), 36 (1997).

[12] B. Julsgaard, J. Sherson, J. I. Cirac, J. Fiurasek, and E. S. Polzik, Nature (London) **432**, 482 (2004).

[13] M. Fleischhauer, A. Imamoglu, and J. P. Marangos, Rev. Mod. Phys. **77**, 633 (2005).

[14] Y.-H. Chen, M.-J. Lee, I.-Chung Wang, S. Du, Y.-F. Chen, Y.-C. Chen, and I. A. Yu, Phys. Rev. Lett. **110**, 083601 (2013).

[15] N. Lauk, C. O'Brien, and M. Fleischhauer, Phys. Rev. A **88**, 013823 (2013).

[16] P. Walther, M. D. Eisaman, A. André, F. Massou, M. Fleischhauer, A. S. Zibrov, and M. D. Lukin, Int. J. Quantum Inform. **05**, 51 (2007).

[17] Igor Vurgaftman and Mark Bashkansky, Phys. Rev. A **87**, 063836 (2013).

[18] L. M. Duan, M. D. Lukin, J. I. Cirac, and P. Zoller, Nature (London) **414**, 413 (2001).

[19] N. Sangouard, C. Simon, H. de Riedmatten, and N. Gisin, Rev. Mod. Phys. **83**, 33 (2011).

[20] Ilse Aben, Wim Ubachs, Pieternel Levelt, Gert van der Zwan, and Wim Hogervorst, Phys. Rev. A **44**, 5881 (1991).

[21] D. A. Steck, Rubidium 87 D Line Data, accessed online at http://steck.us/alkalidata/rubidium87numbers.pdf.

[22] K. F. Reim, J. Nunn, V. O. Lorenz, B. J. Sussman, K. C. Lee, N. K. Langford, D. Jaksch, and I. A. Walmsley, Nat. Photonics **4**, 218 (2010).

[23] H. B. Dang, A. C. Maloof, and M. V. Romalis, Appl. Phys. Lett. **97**, 151110 (2010).

[24] Axel André, Ph.D. thesis, Harvard University, 2005 (unpublished).

[25] Z. Y. Ou, Phys. Rev. A **78**, 023819 (2008).